First clinical description of letermovir resistance mutation in cytomegalovirus UL51 gene and potential impact on the terminase complex structure

Clotilde Muller, Valentin Tilloy, Emilie Frobert, Linda Feghoul, Isabelle Garrigue, Quentin Lepiller, Audrey Mirand, Egor Sidorov, Sébastien Hantz, Sophie Alain

First clinical description of letermovir resistance mutation in cytomegalovirus *UL51* gene and potential impact on the terminase complex structure.

Clotilde Muller[1,*], Valentin Tilloy[2,3], Emilie Frobert [4], Linda Feghoul [5], Isabelle Garrigue [6], Quentin Lepiller [7], Audrey Mirand[8], Egor Sidorov [2], Sébastien Hantz [1,2 £], Sophie Alain[1,2*£]

[1] Univ. Limoges, INSERM, CHU Limoges, RESINFIT, U1092, F-87000 Limoges, France

[2] CHU Limoges, Laboratoire de Bactériologie-Virologie-Hygiène, National Reference Center for Herpesviruses (NRCHV), F-87000 Limoges, France

[3] CHU Limoges, UF9481 Bioinformatique, F-87000 Limoges, France

[4] CHU Lyon, UCL, Virology department, Lyon, France

[5] CHU Saint Louis, AP-HP, Virology department, Paris France

[6] CHU Pellegrin, Virology department, Bordeaux, France

[7] CHU Besançon, Virology department, Besançon, France

[8] CHU Clermont-Ferrand, Virology department, Clermont-Ferrand, France

£ S Hantz and S Alain: equal contribution as co-last author

*Corresponding authors:

clotilde.muller@unilim.fr (C.M.); sophie.alain@unilim.fr (S.A.)

Received: date; Accepted: date; Published: date

Abstract

Background: Letermovir (LMV) is a human cytomegalovirus (HCMV) terminase inhibitor indicated as prophylaxis for HCMV-positive stem-cell recipients. Its mechanism of action involves at least the viral terminase proteins pUL56, pUL89 and pUL51. Despite its efficiency, resistance mutations were characterized *in vitro* and *in vivo*, largely focused on pUL56. To date, mutations in pUL51 in clinical resistance remain to be demonstrated.

Methods: The pUL51 natural polymorphism was described by sequencing 54 LMV-naive strains and was compared to *UL51* HCMV genes from 16 patients non-responding to LMV therapy (prophylaxis or curative). Recombinant viruses were built by «*en-passant*» mutagenesis to measure the impact of the new mutations on antiviral activity and viral growth. Structure prediction was performed by homology modeling. The pUL51 final-model was analyzed and aligned with the atomic coordinates of the monomeric HSV-1 terminase complex (**PDB: 6M5R**).

Results: Among the 16 strains from treated-patients with LMV, 4 never described substitutions in pUL51 (D12E, 17del, A95V, V113L) were highlighted. These substitutions had no impact on viral fitness. Only *UL51*-A95V conferred 13.8-fold increased LMV resistance level by itself (IC50=29.246±0.788).

Conclusion: As an isolated mutation in pUL51 in a clinical isolate can lead to LMV resistance, genotyping for resistance should involve sequencing of the pUL51, pUL56 and pUL89 genes. With terminase modelling, we make the hypothesis that LMV could bind to domains were UL56-L257I and UL51-A95V mutations were localized.

Key words: cytomegalovirus, herpes simplex, letermovir, resistance, terminase, UL51

1. Introduction

Human cytomegalovirus (HCMV) can cause severe complications in immunocompromised patients. The antiviral molecules used against HCMV infection are mainly viral DNA polymerase (pUL54) inhibitors such as, ganciclovir and its prodrug, valganciclovir, cidofovir and foscarnet. The letermovir (LMV) acts via a novel, not fully understood, mechanism involving at least the viral terminase proteins pUL56, pUL89 and pUL51 and therefore offers a different mode of action than anti-polymerase (Ligat et al., 2018; Lischka et al., 2010). Recently recommended as prophylaxis for HCMV infection in high-risk hematopoietic stem cell (HSC) recipients, LMV is occasionally used to treat refractory HCMV infections (Linder et al., 2021; Schubert et al., 2021). Despite its efficiency, resistance mutations were characterized *in vitro* and *in vivo* (Alain et al., 2020; Chou, 2020; Piret and Boivin, 2019). They are largely focused on the protein pUL56 of the terminase complex (Goldner et al., 2011). However, *in vitro* selection experiment with LMV showed the occasional emergence of pUL89 mutations that confer cross-resistance (Chou, 2015). Only one mutation, P91S, was described in the terminase subunit pUL51 by *in vitro* drug selection experiments with LMV (Chou, 2017). To date, this mutation was not found in clinical setting. Samples from patients non-responding to LMV therapy are sent to the National Reference Center (NRC) for Herpeviruses in France for sequencing *UL56*, *UL89, UL51* genes. We reported here the results for 16 LMV-treated patients. By comparison with the *UL51* natural polymorphism obtained after sequencing naïve strains from our collection, we highlighted 4 never described substitutions in pUL51 (D12E, 17del, A95V, V113L). Among them, we report the first resistance mutation described in a clinical sample from a patient under LMV prophylaxis.

To better understand the role of pUL51 in the terminase complex, we defined essential domains by analyzing the pUL51 polymorphism, doing sequence alignments and protein modelling. Moreover, the putative LMV interaction with the terminase complex partners is presented here by analogy with the terminase complex of Herpes Simplex Virus type 1 (HSV-1) (Yang et al., 2020).

2. Materials and methods

2.1. HCMV strains and isolates

Five reference strains – AD169 (**ATCC VR-538**), Davis (**ATCC VR-807**), Towne (**ATCC VR-977**) Merlin (**AY446894.2**) and Toledo (**GU937742.2**) and 72 HCMV DNA samples obtained from clinical isolates or blood samples were analyzed. We included 56 samples from LMV-naïve patients and all the 16 samples from LMV-treated patients collected from 2015 and 2021 in various French hospitals. The 16 blood / plasma samples came from patients receiving LMV in prophylaxis or curative treatment following HSC or solid organ transplantation. They were all sent to the NRC for resistance genotyping. Their viral loads were comprised between 3 and 4.53 log IU.mL^{-1} (median: 3.53; mean: 3.63; SD: ±0.4).

2.2 Amplification and sequencing of *UL56/UL89/UL51* genes from clinical strains

2.2.1. Amplification by nested PCR and Sanger sequencing

The full-length *UL51*, *UL56* and *UL89* genes of all clinical samples were amplified, sequenced and analyzed as previously described for *UL56* and *UL89* (Champier et al., 2008, 2007). Table S1 summarizes the primers and reagents used for amplification and sequencing.

2.2.2 Next generation sequencing and data analysis

UL51 gene coding sequence was amplified by nested PCR for 24 clinical samples from naïve patients and 16 from LMV-treated patients. Viral DNA was isolated from the 32 clinical isolates by the Hirt method (Hirt, 1967). The flowchart of the experiments is presented in Figure 1. A depletion of human DNA was then performed using the NEBNextR Microbiome DNA Enrichment kit (New England Biolabs, Ipswich, USA). Before analysis, all DNAs were purified using magnetic beads (Agencourt AMPure XP) and fragmented using the Ion Xpress Plus DNA Fragment Library Preparation kit (ThermoFisher Scientific, Waltham, USA). Barcodes adapters were ligated to fragment ends and 250 bp fragments were collected. Libraries were PCR amplified, then sequenced either on Ion Proton or S5 machine using Ion Sequencing kit (ThermoFisher Scientific, Waltham, USA). Ubam files from Ion Torrent were converted into fastq using bamtools 2.4.1. Quality check of raw-reads was performed using FastQC v0.11.5 and MultiQC v0.9. A trimming step using Trimmomatic-0.39 was then done using low stringency parameters (phred33 LEADING:3 TRAILING:3 SLIDINGWINDOW:4:15 MINLEN:36 options). Those reads

were then validated using the previous quality check step. Trimmed reads were then aligned against *UL51* sequence exacted from Merlin reference strain (AY446894.2) using BWA-MEM algorithm from Bwa 0.7.17-r1188 and Samtools 1.9 (view, sort and index options). Genetics variations from alignment were called using Lofreq 2.1.3.1. Mutations were then filtered using Bcftools 1.8 based on phred score (200) and depth (100). A filter selecting mutations above 2% allelic frequency was also applied. Consensus files were obtained from VCF files using Bcftools 1.8 (consensus) and formatted using awk custom commands. GenBank accession numbers of the *UL51* sequences range from ON505076 to ON505147.

2.3 Polymorphism and heatmap generation

The binary heatmap provides a data matrix where the colors give an overview of mutational differences between strains. Briefly, the strains groups were extracted from the base dataset and each mutation is recorded in a dummy variable. The base dataset is converted into a 2-dimensional matrix (x, y) with y ordered by the strain and x by the amino acids id. The binary heatmap is plotted showing mutations in saddle brown and absence of a mutation in peach puff. Python 3.9.6 engine is used to generate this binary heatmap (Muller et al., 2021).

2.4 Bacmid recombinant virus assay for characterization of unknown mutations

2.4.1 Cells and bacterial strains

Human fibroblasts MRC-5 (bioMérieux, Marcy l'Etoile, France) were cultivated as previously described **(Jacquet et al., 2020)**. *Escherichia coli* strain GS1783 was used for BAC mutagenesis Bacterial Artificial Chromosome **(Borst et al., 1999)**. The HCMV-BAC contains an enhanced green fluorescent protein (EGFP) gene in the unique short region and was derived from parental strain pHB5, the BAC-cloned genome of the HCMV laboratory strain AD169 **(Chee et al., 1990)** (gift from M. Messerle, Hanover Medical School, Germany).

2.4.2 Antiviral compound

Letermovir was purchased from MedChemExpress (HY-15233), reconstituted in DMSO (Sigma) at 10 mM and stored at −80°C. For antiviral assays, LMV was diluted in cell medium to obtain a final concentration of 40 nM before making serial ½ dilutions down to 1.25 nM. Resistant strains were then tested with a concentration range from 10µM to 10 nM while keeping final DMSO concentrations below 0.1%.

2.4.3 Bacterial Artificial Chromosome mutagenesis

UL51 and *UL56* mutations were introduced by “en passant” mutagenesis into the EGFP-expressing HCMV-BAC and confirmed by sequencing as previously described (Andouard et al., 2016). Primers for mutagenesis are described in Supplementary Table S2.

2.4.5 Antiviral assays and growth curve analysis

Focus reduction assay in 48-well plates was used to assess antiviral susceptibilities to LMV of each mutant as previously described (Jacquet et al., 2020). At least 3 antiviral assays replicates were performed in triplicate for the reference strain AD169 and each mutant HCMV-BAC. The EC50 was determined from EC50 Calculator from AAT Bioquest (https://www.aatbio.com/tools/ic50-calculator). To estimate the impact of each mutation on viral fitness, the recombinant strain and AD169-WT (wild control) were inoculated in 48-well MRC-5 culture at a (MOI) of 0.01. From day 1 to day 7 post-inoculation, number of fluorescent cytopathic foci was counted to establish viral growth curves for each recombinant.

2.5 Identification of conserved patterns and structure prediction

2.5.1 Conserved patterns

The pUL51 amino acids sequence of HCMV reference strain AD169 was first aligned with the homologous proteins from 6 human herpesviruses and then with the sequences of 8 homologous proteins from other beta-herpesviruses, as described in Table S3. Alignments were performed using Clustal Omega multiple sequence alignment (MSA) tools provided by the EMBL-EBI bioinformatics web and programmatic tools framework (Li et al., 2015; McWilliam et al., 2013; Sievers et al., 2011). User-identified structural templates selected from the Protein Data Base (PDB) were used to construct full-length atomic models by iterative template fragment assembly simulations (I-TASSER Protein Structure and Function Prediction program) (Roy et al., 2010; Yang et al., 2015; Yang and Zhang, 2015). Target function was predicted by threading the 3D model through a protein function database. The amino acid sequence of pUL51 HCMV (**P16792.1**) was submitted and the final model with the higher confidence score (c-score) was analyzed using VMD 1.9.4 (Visual Molecular Dynamics).

2.5.2 Tridimensional structure alignment

The atomic coordinates of the monomeric HSV-1 terminase complex (**PDB: 6M5R**) are separated in 3 chains. Chain A corresponds to pUL15 from amino acid T35 to T727, chain B to pUL28 from amino acid A2 to R775 and chain C to pUL33 from amino acid T12 to R129. Atomic coordinates of the chain C were extracted from the text file (**PDB: 6M5R**) with notepad++ (8.1.9.) and were saved in a new file (.txt). The HCMV-pUL51 modelling structure and the new file containing atomic positions of pUL33 from amino acid T12 to R129 were both imported in **VMD 1.9.4**. Analyses were performed using “MultiSeq” analyses. From “Sequence Alignment” function, structures were aligned with “Stamp Structural Alignment”. Both structures are represented with the drawing method “NewCartoon”. Root Mean Square Deviation **(RMSD)** score of atomic position was analyzed in Excel (Figure S1). In the same way, HCMV-pUL51

modelling structure was aligned with HSV-1 pUL33 structure in the whole HSV-1 terminase complex (**PDB: 6M5R**). The Chain C of HSV-1 terminase complex was selected to do "Sequence alignment" and "Stamp Structural Alignment".

3. Results

3.1. Identification of polymorphisms

The *UL51* sequencing results of reference strains AD169, Towne and Toledo were identical to the sequences found in the GenBank (accession number **FJ527563.1**, **GQ121041.1**, **GU937742**) by both methods used (Sanger and NGS). Thus, inter-assay reproducibility was 100%. Among the 56 LMV-naïve strains, 14 amino acid polymorphisms were distributed across pUL51 (Figure 2). Only one substitution (S153P) was also present in the reference strains Towne, Toledo, Davis and Merlin but not in AD169. The main identity of the HCMV isolates was 98.96% (range 97.45% to 100%) and the mean number of polymorphisms per isolates was 1.6 (range 0 to 4). Analysis of polymorphisms repartition through pUL51 revealed a huge concentration of amino acid substitution in a N-terminal part. Single nucleotide polymorphisms (SNPs) of 56 LMV-naïve strains did not concern the C-terminal part except for the S153P substitution found also in reference strains Towne, Toledo, Davis and Merlin. Among the 16 LMV-treated samples, 15 were sequenced by NGS method. For the remaining sample which had a low DNA concentration, only the Sanger sequence was used (Figure 1). Eight SNPs were found: 1 was common to reference strains (S153P), 3 to LMV-naive strains (A4T, G16A, Q23K) and 4 had never been described (D12E; 17del; A95V; V113L). D12E and 17del are in the high natural polymorphism part; A95V and V113L substitutions are in a polymorphism-free part. These 4 residues were found in samples collected from 4 different patients. The patient's sample harboring the A95V substitution on pUL51 has the L257I substitution in pUL56. This patient was a stem cell recipient and developed HCMV reactivation under LMV-prophylaxis. Both patient's samples harboring the D12E or V113L substitutions on pUL51 have respectively the C325F or C325Y substitution in pUL56. At least, the patient's sample harboring the 17del in pUL51 was not associated with any mutation in pUL56. UL89 gene sequences of these four patient's samples were similar to the reference strain (Table 1).

3.2. Phenotypic characterization of newly detected mutations

Genotypes and phenotypes of recombinant-viruses representing the newly detected mutations are summarized in Table 2. The UL51 D12E, 17del and V113L mutations did not confer resistance to LMV, while UL51-A95V confers a 13.8-fold increase of the EC50 of LMV (EC50=29.246±0.788). Double mutants were constructed according patient's samples genotyping (Table 1) to study the effect of the UL51 substitutions in combination with UL56

substitutions (Table 2). Results indicated that the combined mutations UL51-A95V and UL56-L257I confers a 127.7-fold increase LMV resistance (EC50=271.39±41.05). For both double mutants UL51-D12E / UL56-C325F and UL51-V113L / UL56-C325W the EC50 is greater than 10 µM (Table 2).

3.3. Effect of mutations on viral growth

The assessment of the impact on viral fitness of each mutation was compared with the parental strain AD169-WT. Mutations in recombinant viruses had no significant impact on viral fitness except for the double AD169 UL51-A95V / UL56-L257I (Figure 3).

3.4. Identification of conserved regions

Alignment of 6 human herpesviruses pUL51 homologs (Table S3) allows to highlight 2 parts in the protein; the N-terminal side which does not seem to be conserved and the C-terminal side showing a higher degree of conservation (Figure 4, A). To further determine conserved regions, homologs of HCMV pUL51 protein were studied in 8 beta-herpesviruses (Table S3). Amino acids alignment shows 37 residues as strictly similar, 25 strongly similar and 5 weakly similar. All conserved residues are found in the C-terminal part of the sequence alignments from amino acid Y86 to E148 (Figure 4, B). The resistance mutation UL51-A95V affects a strictly conserved residue of the conserved part in both human and beta-herpesviruses alignments. N-terminal part shows gaps or variability between residues, which is characteristic of a variable region.

3.5. Tridimensional modelling of pUL51 and alignment with pUL33 from the terminase complex of HSV-1

To identify the tridimensional amino acids position, protein modelling was performed with I-TASSER. The predicted secondary structure is mainly composed of helices on the C-terminal part. The N-terminal part is mostly composed of coils, with some helices. The I-TASSER report suggested the presence of a possible ligand binding sites in the C-terminal part. These initial structural data were consistent with the “conclusions” drawn from polymorphism analysis and alignments. The three-dimensional structure of the HSV-1 packaging complex was elucidated in 2020 by cryo-electron microscopy (Yang et al., 2020). In order to validate the modelling of pUL51 determined by I-TASSER, structure alignment was performed after the pUL33 coordinates extraction from the PDB file (**PDB: 6M5R**). Superposition of the cryo-electron microscopy structure of HSV-1 pUL33 and HCMV pUL51 modelling structure showed strong similarities in the C-terminal part of both proteins (RMSD scoring in Figure S1). As anticipated, differences observed were pronounced in the N-terminal part determined as a variable region with polymorphism and protein alignment studies (Figure 4).

Strains of studied patients possessed mutations in both proteins pUL56 and pUL51. The HCMV pUL51 protein structure was aligned with pUL33 in the whole HSV-1 terminase complex. Thus, pUL51 mutations can be reported in the model (Figure 5). To identify the location of the pUL56 resistance mutations in HSV-1 terminase model, amino acid sequences of pUL56 and HSV-1 pUL28 were aligned together (Figure S2). pUL56 mutated residues were reported in pUL28: for example, the corresponding amino acid of the mutation L257I in pUL56 corresponds to the residue D253 in pUL28. The Figure 5 presents HSV-1 terminase model where pUL51 was structurally aligned with pUL33. In the HSV-1 terminase model, the location HCMV-UL51-A95 residue is very close from the HSV-1-UL28-D253 in the tridimensional space, corresponding to HCMV-UL56-L257 (Figure 6).

4. Discussion

pUL51 has been shown to be essential for viral replication and the normal packaging function of the terminase complex (Borst et al., 2013). LMV targets the terminase complex, however its mechanism of action remains to be elucidated. A resistance mutation (P91S) emerged by *in vitro* experiment in pUL51 under LMV pressure selection (Chou, 2017). Although not yet implemented in the clinical setting, we decided to sequence this gene in addition to *UL56* and *UL89* genes for non-responder patient receiving LMV. To identify putative resistance mutations in pUL51, we determined the *UL51* natural polymorphism by sequencing from 56 LMV-naïve patients. Working from clinical samples or isolates, we used NGS sequencing results, in order to detect minority variants. Sensitivity of the NGS method for minority mutants was previously determined between 2-5% in these conditions (personal unpublished data). Natural polymorphism is largely located in the N-terminal part of the protein from the amino acid 4 to the amino acid 70 with one mutation in the C-terminal part (S153P). Sequences alignments with pUL51 homologs from both human-herpesviruses and beta-herpesviruses revealed a variable part in N-terminal and a conserved region in C-terminal from the amino acid Y86 to E158 suggesting the importance of this part for pUL51 structure-function. The difference between pUL51 homologs is due to the N-terminal part size. These results are consistent with previous works that argued that the pUL51 C-terminal part is crucial for terminase complex assembly (Borst et al., 2013; Neuber et al., 2018, 2017). The comparison of natural polymorphisms map with the 16 sequences from LMV-treated patients evidenced 4 new mutations both detected by Sanger and NGS analysis (D12E, 17del, A95V, V113L).

The A95V substitution affects an alanine in position 95 completely conserved among herpesviruses suggesting the importance of this residue (Figure 3). Alanine 95 is located at the beginning of the **helix 5** (Figure 5). The A95V change conserved the aliphatic characteristic of the amino acid and did not affect the viral growth (Figure 3). However, this substitution may

induce conformational changes because of the additional CH3-group of valine. It could affect the interaction of LMV with specific amino acids, as the EC50 increases by 13.8-fold (Table 2). Described by Chou in 2017, the substitution P91S confers a 3.8-fold increase in LMV EC50 (Chou, 2017). The proline 91 is strictly conserved in herpesviruses as A95. P91 is located in a small region that could form a coil between the helices 4 and 5 (Figure 5). These mutations, very close to each other, both confer resistance to LMV by their own. The residue V113 is also located in the high conserved region; this amino acid is strictly conserved in beta-herpesviruses studied (Figure 4). The substitution V to L does not change its aliphatic characteristic and did not affect the viral growth. Moreover, V113L substitution does not confer by itself a resistance to LMV. Finally, D12E and 17del substitutions are located in the high polymorphism part and are non-conserved among herpesviruses (Figure 2 and 4). Both mutations do not influence the viral growth nor confer any resistance to LMV (Table 2, Figure 3).

Double mutant viruses were built to study the effect of the *UL51* substitutions in combination with *UL56* substitutions. The UL56-L257I and UL51-A95V double mutants showed an EC50 of 271.39±41.05 nM. UL56-L257I was previously characterized and conferred 4- to 15-fold change in LMV EC50 (Chou, 2017). Thus, the combination of these both mutations largely increases the resistance to LMV (fold-change = 127.833) (Table 2). Both UL56-C325F and UL56-C325W mutations, already characterized, showed an EC50 ratio > 3000 (Chou, 2020, 2015). The addition of the UL51-D12E and UL51-V113L to UL56-C325F and UL56-C325W, respectively, do not modify the level of resistance of pUL56 resistant mutations (Table 2). Indeed, for these both double mutants, the EC50 ratio is higher than 3000. Thus, these results do not allow to know whether the combination of these mutations further increases LMV resistance. A substitution on the residue 17 was observed in a LMV-naïve strain (E17A). Due to the position in the high polymorphism part and the result associated to recombinant viruses, we can consider that UL51-D12E and UL51-17del are polymorphism substitutions.

Mutations conferring LMV resistance in the pUL89, pUL56, and pUL51 proteins were plotted in the model to gain insight into their localization (Figure 7). The resistance mutations in pUL56 and pUL51 reported in the model are localized in a very small area of the complex. Due to the differences of sequences between HSV-1 and HCMV proteins, pUL56 residues S229, V231, N232, V236, E237 conferring a resistance to LMV cannot be reported in the model (Figure 7). The pUL89 resistance mutations reported in HSV-1 pUL15 appear to be distant from the pUL56 mutations (Figure 7, Figure S3). However, as the complex assembles in hexamer and dodecamer, the region of pUL89 where the mutations localized could be close to the region harboring the mutations in pUL56 and pUL51 (Yang et al., 2020). Although functional domains of herpesviruses are conserved, LMV has no activity on HSV-1. This is probably due to differences

of size and conformation of the proteins forming the terminase complex as demonstrated by alignment of pUL56 and pUL28 and localization of resistance mutations on this alignment (Figure S2 and S3). Nevertheless, this model allows to better understand how the LMV could interact with pUL56, pUL51 and pUL89 and disrupt their interaction. All described resistance mutations could potentially block LMV fixation in a pocket formed by all 3 proteins of the complex. It could explain why the resistance mutations of pUL56 are not only localized in conserved regions contrary to what is classically described for other antiviral targets (Chou et al., 2003).

Conclusion

We herein confirm the role of pUL51 mutations in LMV resistance in the clinical setting and describe the first resistance mutation in a LMV-treated patient. As a single mutation in pUL51 can lead to LMV resistance with a 13.8-fold increase in EC50, it is essential to systematically sequence the 3 genes encoding the complex terminase. Moreover, a combination of mutations in pUL56 or pUL51 can multiply the level of LMV resistance by 127.8-fold. By terminase modelling, we make the hypothesis that LMV could bind to the domain where both P91S and A95V substitutions were localized. Moreover, we can make the hypothesis that the domains including both UL56-L257 and UL51-P91 and UL51-A95 could be involved in LMV interaction with the HCMV terminase complex as combined mutations can increased the level of resistance to LMV.

Author Contributions

Author Contributions: CM performed experiments, tridimensional and statistical analyses, wrote the manuscript, and prepared the figures. VT participated in research experiments and bioinformatics analysis for NGS. SA provided naïve samples and strains and coordinated the polymorphism study from clinical samples. EF, LF, IG, QL, AM provided the 16 resistant samples, to the NRC and reviewed the manuscript. SA and SH designed the research, coordinated the research and manuscript writing.

Acknowledgments:

The authors acknowledge Melissa Mayeras and Mathieu Lafarge from the technical facilities and clinicians from French hospitals for their assistance. We thank Gaëtan Muller for his expertise in bioinformatics.

Figure 1: Flow chart of the sequencing analysis. 56 (32+24) clinical samples came from patients naive of LMV (either congenitally infected newborns or immunocompromised patients)

and 16 clinical samples from LMV non responding patients. UL51 sequences amplified by nested PCR were sequenced by both Sanger and NGS. LMV: letermovir, PCR : polymerase chain reaction, * low amount of DNA.

Figure 2: Polymorphism distribution of HCMV pUL51. (A) Representation through a binary heatmap of the polymorphism distribution according to the strain and the position of the mutation in pUL51. The 3 groups studied (reference strains (n = 5), naïve strains (n = 54) and strains from patients treated with LMV (n = 16) are represented by black, grey and saddle brown, respectively, in the y axis. Mutations are shown in saddle brown and the absence of a mutation in peach puff. **(B)** Description of the polymorphism mutation depending on the group. LMV: letermovir; aa: amino acids.

Table 1: Characteristics of the clinical samples.

Table 2: Effective Concentration 50% of viral growth (EC50) obtained for the recombinant viruses.

Figure 3: Growth curves analysis of the recombinant viruses. (A) Growth curves of the recombinant virus strain AD169 UL51 D12E and AD169 UL51 D12E UL56 C325F in comparison to the parental strain AD169 WT. **(B)** Growth curves of the recombinant virus strain AD169 UL51 A95V and AD169 UL51 A95V-UL56 L257I in comparison to the parental strain AD169 WT. **(C)** Growth curves of the recombinant virus strain AD169 UL51 V113L and AD169 UL51 V113L UL56 C325Y in comparison to the parental strain AD169 WT. **(D)** Growth curves of the recombinant virus strain AD169 UL51 17del in comparison to the parental strain AD169 WT. Fluorescent foci were counted daily from day 1 to day 7. Curves are the average of four independent experiments in triplicate. Mann-Whitney test was applied for statistical analysis: recombinant strains were compared to the parental strain. * $p < 0.05$, ** $p < 0.01$, *** $p < 0.001$.

Figure 4: Sequence alignment of the pUL51 homologs in human herpesviruses (A) and beta-herpesviruses (B). Mutations found to be novel in HCMV strains from treated patients compared to the pUL51 natural polymorphism are shown in white letters on a red background (D12E, 17del, A95V, V113L). The P91S mutation described by Chou et al, 2017 is also represented in white letters on a red background. The degree of amino acid conservation is represented as follows: "*" indicates a strictly conserved amino acid; ":" a site belonging to a group exhibiting strong similarity; "." a site belonging to a group exhibiting a weak similarity.

Figure 5: Atomic structure of HCMV pUL51 and HSV-1 pUL33. (A) Modelling structure of the HCMV pUL51 protein using I-TASSER reports a protein composed at least of 6 helices (α1 to α6)

and a strand (β1). (B) Cryo-electron microscopy structure of the HSV-1 pUL33, consisting of 5 helices (α1 to α5). (C) Structure superposition of the both proteins. Superposition of the proteins shows a higher atomic divergence for the N-terminal part. The atomic position of pUL33 residues was extracted from the PDB file 6M5R. Structures are represented with the drawing method "NewCartoon" using Visual Molecular Dynamics (VMD 1.9.3). HSV-1 pUL33 and HCMV pUL51 are respectively colored in red and pink. aa : amino acid, α : helix, β : strand.

Figure 6: Atomic structure of HSV-1 terminase complex. Cryo-electron microscopy structure of the HSV-1 terminase complex including HCMV-pUL51 protein structure instead of HSV-1-pUL33. Zoom of the part with both mutations found in pUL51 and the reported mutation in HSV-1-pUL28. Visualization of the structures was performed using Visual Molecular Dynamics (VMD 1.9.3). pUL15 (HSV-1), pUL28 (HSV-1) and pUL51 (HCMV) are represented in NewCartoon and colorized in grey, cyan and pink respectively. Residue implicated in a mutation are represented in VDW and colorized in blue for pUL28 and in green for pUL51. pUL28 D253 correspond to pUL56 L257.

Figure 7: Atomic structure of HSV-1 terminase complex comprising reported letermovir mutation. (A) Cryo-electron microscopy structure of the HSV-1 terminase complex including HCMV-pUL51 protein structure instead of HSV-1-pUL33. pUL15, pUL28 and pUL51 are represented in NewCartoon and colorized in grey, cyan and pink respectively. Residues implicating a letermovir resistance in pUL56, pUL89 are reported in pUL28 and pUL15 as described in the table. Residues implicating a letermovir resistance in pUL51 are directly reported in the structure. They are represented in "VDW" and colorized in blue, orange and green, respectively. (B) Amino acid correspondence of resistance mutations described in pUL56 and pUL89 **(Piret et al., 2019; Chou 2020)**

References

Alain, S., Feghoul, L., Girault, S., Lepiller, Q., Frobert, E., Michonneau, D., Berceanu, A., Ducastelle-Lepretre, S., Tilloy, V., Guerin, E., Le Goff, J., Peytavin, G., Hantz, S., 2020. Letermovir breakthroughs during the French Named Patient Programme: interest of monitoring blood concentration in clinical practice. J Antimicrob Chemother 75, 2253–2257. https://doi.org/10.1093/jac/dkaa135

Andouard, D., Mazeron, M.-C., Ligat, G., Couvreux, A., Pouteil-Noble, C., Cahen, R., Yasdanpanah, Y., Deering, M., Viget, N., Alain, S., Hantz, S., 2016. Contrasting effect of new HCMV pUL54 mutations on antiviral drug susceptibility: Benefits and limits of 3D analysis. Antiviral Research 129, 115–119. https://doi.org/10.1016/j.antiviral.2016.02.004

Borst, E.-M., Hahn, G., Koszinowski, U.H., Messerle, M., 1999. Cloning of the Human Cytomegalovirus (HCMV) Genome as an Infectious Bacterial Artificial Chromosome in Escherichia coli: a New Approach for Construction of HCMV Mutants. J. VIROL. 73, 10.

Borst, E.M., Kleine-Albers, J., Gabaev, I., Babić, M., Wagner, K., Binz, A., Degenhardt, I., Kalesse, M., Jonjić, S., Bauerfeind, R., Messerle, M., 2013. The Human Cytomegalovirus UL51 Protein Is Essential for Viral Genome Cleavage-Packaging and Interacts with the Terminase Subunits pUL56 and pUL89. Journal of Virology 87, 1720–1732. https://doi.org/10.1128/JVI.01955-12

Champier, G., Couvreux, A., Hantz, S., Rametti, A., Mazeron, M.-C., Bouaziz, S., Denis, F., Alain, S., 2008. Original article Putative functional domains of human cytomegalovirus pUL56 involved in dimerization and benzimidazole D-ribonucleoside activity. Antiviral Therapy 12.

Champier, G., Hantz, S., Couvreux, A., Stuppfler, S., Mazeron, M.-C., Bouaziz, S., Denis, F., Alain, S., 2007. New functional domains of human cytomegalovirus pUL89 predicted by sequence analysis and three- dimensional modelling of the catalytic site DEXDc. Antiviral Therapy 16.

Chee, M.S., Bankier, A.T., Beck, S., Bohni, R., Brown, C.M., Cerny, R., Horsnell, T., Hutchison, C.A., Kouzarides, T., Martignetti, J.A., 1990. Analysis of the protein-coding content of the sequence of human cytomegalovirus strain AD169. Curr Top Microbiol Immunol 154, 125–169. https://doi.org/10.1007/978-3-642-74980-3_6

Chou, S., 2020. Advances in the genotypic diagnosis of cytomegalovirus antiviral drug resistance. Antiviral Research 176, 104711. https://doi.org/10.1016/j.antiviral.2020.104711

Chou, S., 2017. A third component of the human cytomegalovirus terminase complex is involved in letermovir resistance. Antiviral Research 148, 1–4. https://doi.org/10.1016/j.antiviral.2017.10.019

Chou, S., 2015. Rapid *In Vitro* Evolution of Human Cytomegalovirus UL56 Mutations That Confer Letermovir Resistance. Antimicrobial Agents and Chemotherapy 59, 6588–6593. https://doi.org/10.1128/AAC.01623-15

Chou, S., Lurain, N.S., Thompson, K.D., Miner, R.C., Drew, W.L., 2003. Viral DNA Polymerase Mutations Associated with Drug Resistance in Human Cytomegalovirus. The Journal of Infectious Diseases 188, 32–39. https://doi.org/10.1086/375743

Goldner, T., Hewlett, G., Ettischer, N., Ruebsamen-Schaeff, H., Zimmermann, H., Lischka, P., 2011. The Novel Anticytomegalovirus Compound AIC246 (Letermovir) Inhibits Human Cytomegalovirus Replication through a Specific Antiviral Mechanism That Involves the Viral Terminase. Journal of Virology 85, 10884–10893. https://doi.org/10.1128/JVI.05265-11

Hirt, B., 1967. Selective extraction of polyoma DNA from infected mouse cell cultures. Journal of Molecular Biology 26, 365–369. https://doi.org/10.1016/0022-2836(67)90307-5

Jacquet, C., Marschall, M., Andouard, D., El Hamel, C., Chianea, T., Tsogoeva, S.B., Hantz, S., Alain, S., 2020. A highly potent trimeric derivative of artesunate shows promising treatment profiles in experimental models for congenital HCMV infection in vitro and ex vivo. Antiviral Research 175, 104700. https://doi.org/10.1016/j.antiviral.2019.104700

Li, W., Cowley, A., Uludag, M., Gur, T., McWilliam, H., Squizzato, S., Park, Y.M., Buso, N., Lopez, R., 2015. The EMBL-EBI bioinformatics web and programmatic tools framework. Nucleic Acids Research 43, W580–W584. https://doi.org/10.1093/nar/gkv279

Ligat, G., Cazal, R., Hantz, S., Alain, S., 2018. The human cytomegalovirus terminase complex as an antiviral target: a close-up view. FEMS Microbiology Reviews 42, 137–145. https://doi.org/10.1093/femsre/fuy004

Linder, K.A., Kovacs, C., Mullane, K.M., Wolfe, C., Clark, N.M., La Hoz, R.M., Smith, J., Kotton, C.N., Limaye, A.P., Malinis, M., Hakki, M., Mishkin, A., Gonzalez, A.A., Prono, M.D., Ostrander, D., Avery, R., Kaul, D.R., 2021. Letermovir treatment of cytomegalovirus infection or disease in solid organ and hematopoietic cell transplant recipients. Transplant Infectious Disease 23. https://doi.org/10.1111/tid.13687

Lischka, P., Hewlett, G., Wunberg, T., Baumeister, J., Paulsen, D., Goldner, T., Ruebsamen-Schaeff, H., Zimmermann, H., 2010. *In Vitro* and *In Vivo* Activities of the Novel Anticytomegalovirus Compound AIC246. Antimicrobial Agents and Chemotherapy 54, 1290–1297. https://doi.org/10.1128/AAC.01596-09

McWilliam, H., Li, W., Uludag, M., Squizzato, S., Park, Y.M., Buso, N., Cowley, A.P., Lopez, R., 2013. Analysis Tool Web Services from the EMBL-EBI. Nucleic Acids Research 41, W597–W600. https://doi.org/10.1093/nar/gkt376

Muller, C., Alain, S., Gourin, C., Baumert, T.F., Ligat, G., Hantz, S., 2021. New Insights into Human Cytomegalovirus pUL52 Structure. Viruses 13, 1638. https://doi.org/10.3390/v13081638

Neuber, S., Wagner, K., Goldner, T., Lischka, P., Steinbrueck, L., Messerle, M., Borst, E.M., 2017. Mutual Interplay between the Human Cytomegalovirus Terminase Subunits pUL51, pUL56, and pUL89 Promotes Terminase Complex Formation. Journal of Virology 91. https://doi.org/10.1128/JVI.02384-16

Neuber, S., Wagner, K., Messerle, M., Borst, E.M., 2018. The C-terminal part of the human cytomegalovirus terminase subunit pUL51 is central for terminase complex assembly. Journal of General Virology 99, 119–134. https://doi.org/10.1099/jgv.0.000984

Piret, J., Boivin, G., 2019. Clinical development of letermovir and maribavir: Overview of human cytomegalovirus drug resistance. Antiviral Research 163, 91–105. https://doi.org/10.1016/j.antiviral.2019.01.011

Roy, A., Kucukural, A., Zhang, Y., 2010. I-TASSER: a unified platform for automated protein structure and function prediction. Nature Protocols 5, 725–738. https://doi.org/10.1038/nprot.2010.5

Schubert, L., Fisecker, L., Thalhammer, F., Burgmann, H., Steininger, C., 2021. Letermovir for the compassionate therapeutic use of cytomegalovirus infection. Eur J Clin Microbiol Infect Dis 40, 435–439. https://doi.org/10.1007/s10096-020-03990-w

Sievers, F., Wilm, A., Dineen, D., Gibson, T.J., Karplus, K., Li, W., Lopez, R., McWilliam, H., Remmert, M., Söding, J., Thompson, J.D., Higgins, D.G., 2011. Fast, scalable generation of high-quality protein multiple sequence alignments using Clustal Omega. Molecular Systems Biology 7, 539. https://doi.org/10.1038/msb.2011.75

Yang, J., Yan, R., Roy, A., Xu, D., Poisson, J., Zhang, Y., 2015. The I-TASSER Suite: protein structure and function prediction. Nature Methods 12, 7–8. https://doi.org/10.1038/nmeth.3213

Yang, J., Zhang, Y., 2015. I-TASSER server: new development for protein structure and function predictions. Nucleic Acids Research 43, W174–W181. https://doi.org/10.1093/nar/gkv342

Yang, Y., Yang, P., Wang, N., Chen, Z., Su, D., Zhou, Z.H., Rao, Z., Wang, X., 2020. Architecture of the herpesvirus genome-packaging complex and implications for DNA translocation. Protein & Cell 11, 339–351. https://doi.org/10.1007/s13238-020-00710-0

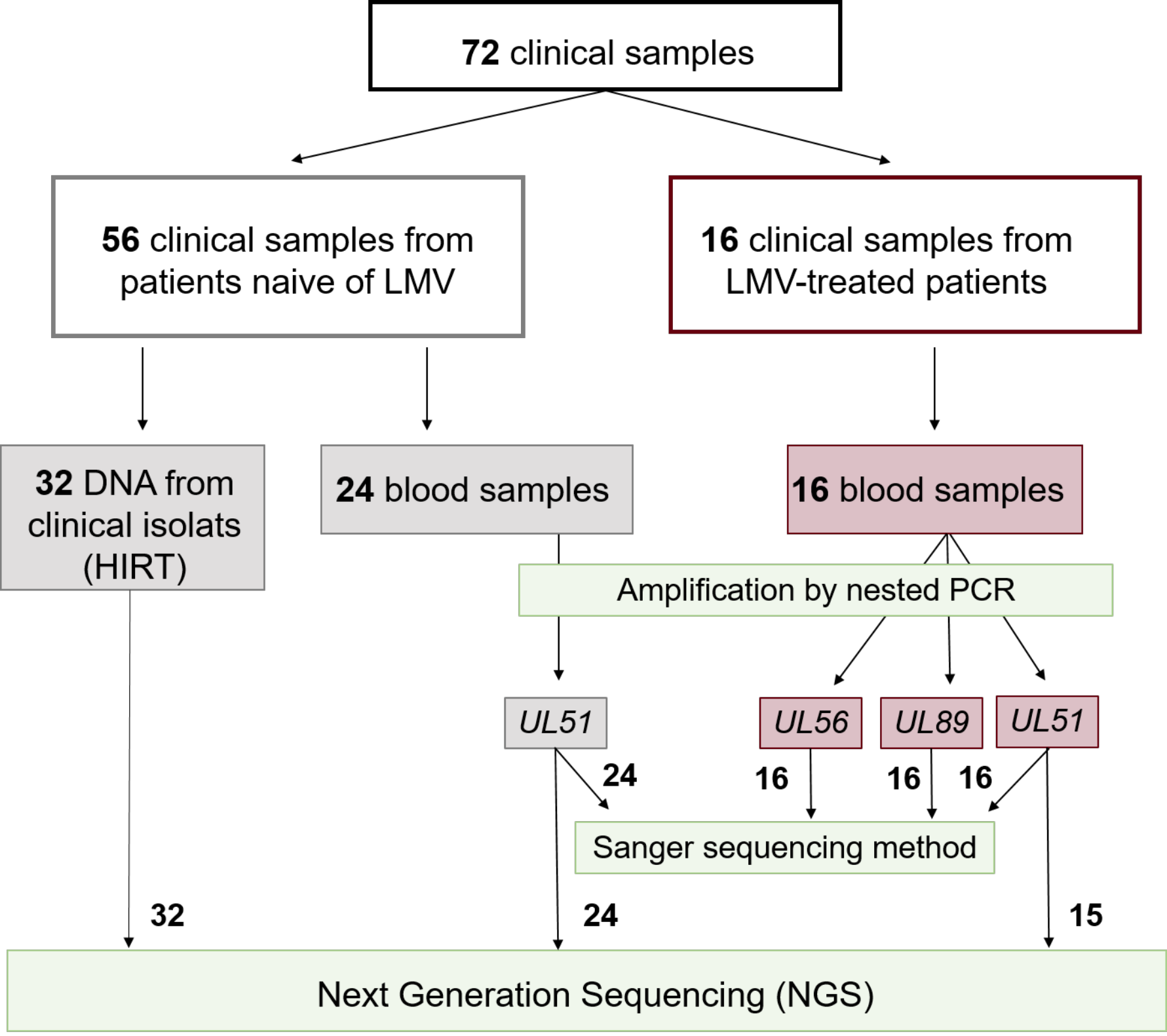
72 clinical samples
56 clinical samples from patients naive of LMV
16 clinical samples from LMV-treated patients
32 DNA from clinical isolats (HIRT)
24 blood samples
16 blood samples
Amplification by nested PCR
UL51
UL56
UL89
UL51
24
16
16
16
Sanger sequencing method
32
24
15
Next Generation Sequencing (NGS)

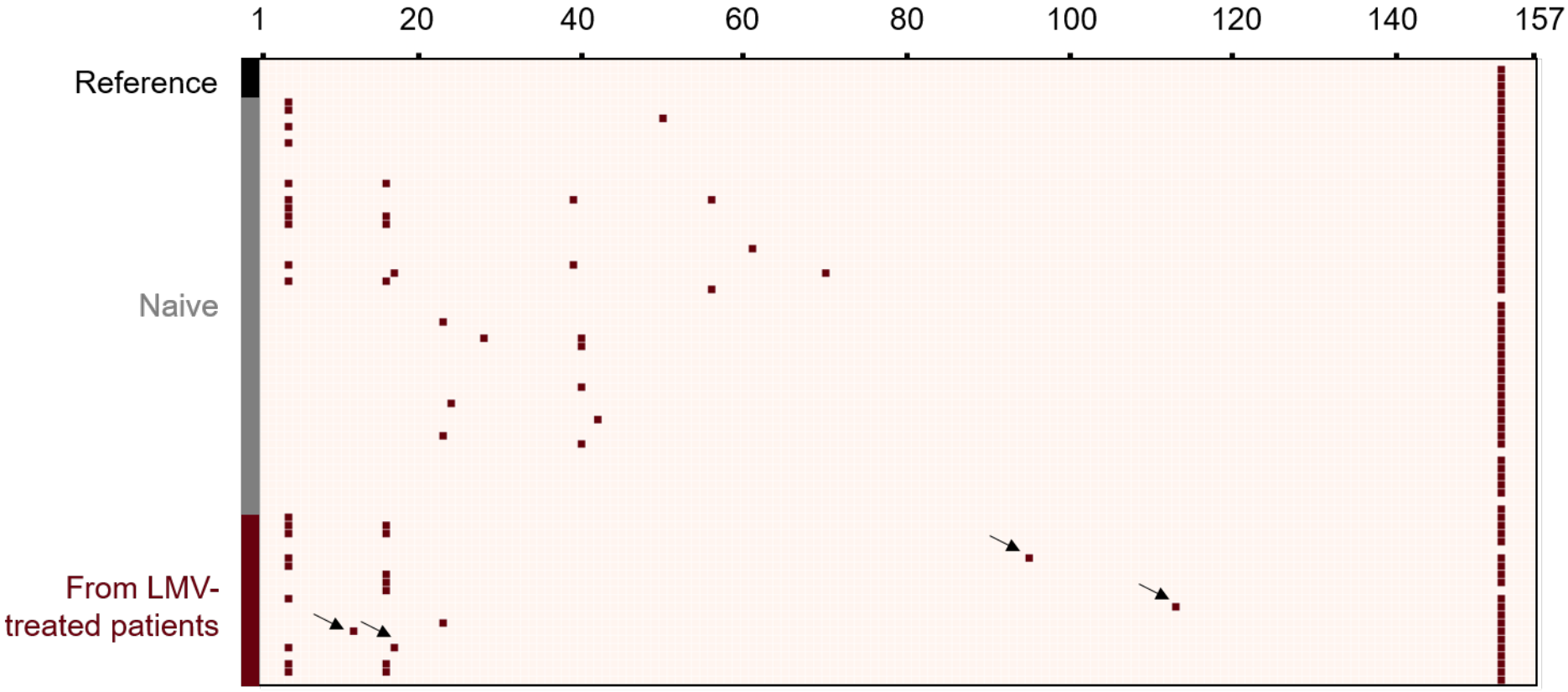

Reference strains (n=5)	S153P
Clinical naive strains (n=56)	A4T, G16A, E17A, Q23K, D24G, S28F, E39D, D40N, E42G, G56D, G61D, L70I
Clinical strains from treated patients (n=16)	**D12E, A95V, V113L, 17del**

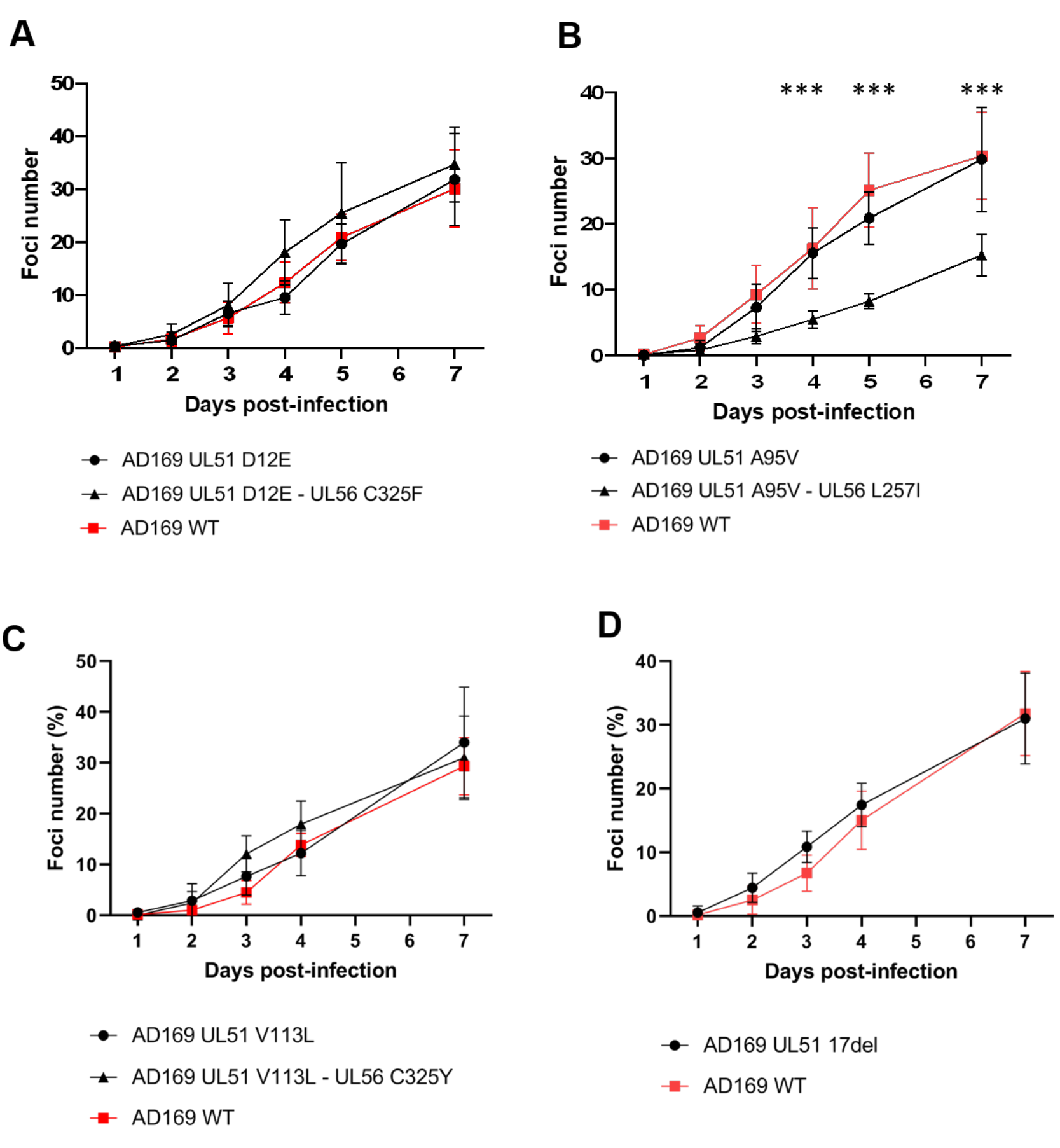
A
Foci number
Days post-infection
AD169 UL51 D12E
AD169 UL51 D12E - UL56 C325F
AD169 WT
B
***
***
***
Foci number
Days post-infection
AD169 UL51 A95V
AD169 UL51 A95V - UL56 L257I
AD169 WT
C
Foci number (%)
Days post-infection
AD169 UL51 V113L
AD169 UL51 V113L - UL56 C325Y
AD169 WT
D
Foci number (%)
Days post-infection
AD169 UL51 17del
AD169 WT

A

Human herpesviruses

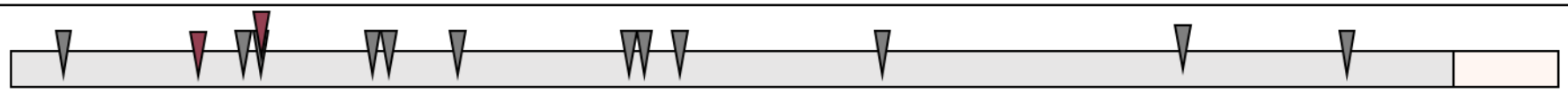

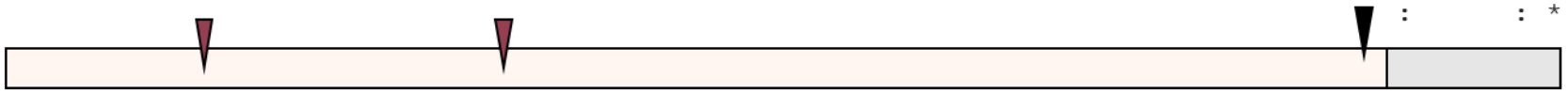

```
HSV-1   ------------------------------------------MAGREG---RTRQRTLRDTIPDCALRSQTLESLDARYVSRDGAHDAAVWFEDMT-
HSV-2   ------------------------------------------MAGRAG---RTRPRTLRDAIPDCALRSQTLESLDARYVSRDGAGDAAVWFEDMT-
VZV     ---------MYESENASEHHPELEDVFSE--------NTGDSNPSMGSSDSTRSISGMRARDLITDTDVNLLNIDALESKYFPADSTFTLSVWFENLI-
HCMV    MSWAKQRVPFLDDDDGEE-ENDVQDDVDSPVPTRPLVIDEDAEPAAGTSGGLEGGGGDD-------------EDGEDGH-ALPDLDDDLLLQFEPML-
HHV-6A  ------------------------------------MDS--SPEKT-------------------------NLELLYE-RFCEQGREFEVVFYPML-
HHV-6B  ------------------------------------MMDS--SPEKT-------------------------NLELLYE-QVCEQGREFEVVFYPML-
EBV     ------------------------------------------MTHLGGKVRSSGFLIPGSAPVSGTPPQGQGGLASSRVYEDSGGS-LLSFSPMIH

HSV-1   PAELEVVFPTTDAKLNYLSRTQRLASLLTYAGPIKAPDDAAAPQTPDTACVHGELLARKRERFAAVINRFLDLHQILRG--------------  130
HSV-2   PAELEVIFPTTDAKLNYLSRTQRLASLLTYAGPIKAPDGPAAPHTQDTACVHGELLARKRERFAAVINRFLDLHQILRG--------------  130
VZV     PPEIEAILPTTDAQLNYISFTSRLASVLKHKESNDS-----EKSAYVVPCEHSASVTRRRERFAGVMAKFLDLHEILKDA-------------  156
HCMV    PRVYDLLLPSLDARLNFVNAGQKYAAFLKYVH-----------GDCATCSHGEILREKTQLLTAIVSKLMDINGILEGKDEPAPGK-------  157
HHV-6A  PRLYEMMLPSLEARLNFLSVGYRHVAFARYVH-----------GDV-DCVHREVMAQKMVLLTSILSKLLNVNGILEHQEYLNTE--------  105
HHV-6B  PRLYEMMLPSLEARLNFLSVGYRHVAFSRYVH-----------GDV-DCVHREVMAQKMVLLTSILSKLLNVNGILEHQEYLNTE--------  106
EBV     PNLAPLIAPSAYARLNLLNHCIFLEAFKEEN-----------SGQGLGGVQREVLFLKRDIIKQVIARIVAADSTLDLVNHGEPGREAPRRAQ  135
```

B

Beta-herpesviruses

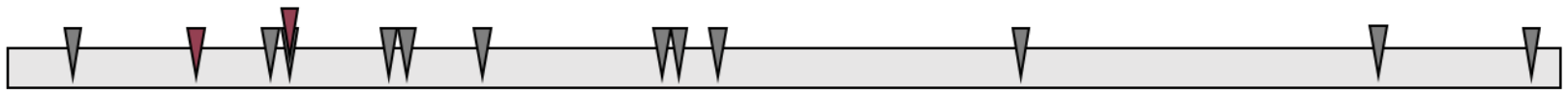

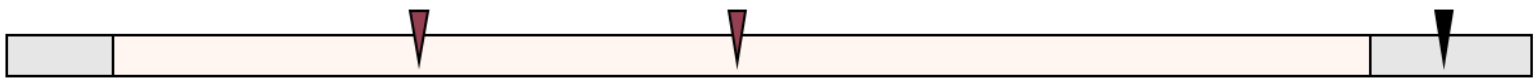

```
AoHV-1      ------------------------------------------------------------------------------MSEEENGEQEPQEA
HCMV        MSWAKQRVPFLDDDDGEEENDVQDDVDSPVPTRPLVIDEDAEP----AAGTSGGLEGGGGD----------------DEDGEDGHALPDLD
PnHV-2      MA----------TLRG-------RETTTPSPPPPQLGGEDPGREVDDYKGGEGRFEVDDSRDDDGEDSPSSSVPPPLVIDEDAEYGLGEAE
RhCMV       ------------------------------------------------------------MASFRSARAVHREDPDDDEDGTLDPE
CyCMV       ------------------------------------------------------------MASFRSARVVHGEDPDDDEDGTLDPE
BCMV        ----------------------------------------------------------------MAARRDREDAYEDGFLDPD
CeHV-5      --------------------------------------------------------------MAAPSARLDQDDPYDEGLFEPD
BatBHV-2    ---------------------------------------------MS---AGDDGGR-------------DGERAGLCRFYDELMLDV
TuHV-1      ------------------------------------------MDDVSG---AEDVGGGR---GVA-AAAALPPPPDEFPVAFEPMLPRV

AoHV-1      EEPYVKFEPMLPKLYELLLPSLDARLNFVNAGQKHAAFFKYVYGQRATCSHAEILCSKTKLLTAIVAKLMDINGILEEKDESG---  97
HCMV        DDLLLQFEPMLPRVYDLLLPSLDARLNFVNAGQKYAAFLKYVHGDCATCSHGEILREKTQLLTAIVSKLMDINGILEGKDESAPGK  157
PnHV-2      DDLLVQFEPMLPRVYDLLLPSLDARLNFVNAGQKYAAFLKYVHGECASCSHGQILREKTQLLTAIVTKLMDINGILEGKDELASGK  160
RhCMV       DELEVSFEPMLPRVYELMLPSLDARLNFINAGQKYAAFLKYVHGECSSCNHAQILNEKTKLLTAIVNKLMDINGILEGKEESAGK-  111
CyCMV       DELEVSFEPMLPRVYELMLPSLDARLNFINAGQKYAAFLKYVHGECSSCNHAQILNEKTKLLTAIVNKLMDINGILEGKEESAGK-  111
BCMV        EDFEVSFEPMLPRVYELLLPSLDARLNFVNAGQKYAAFLKYVHGECSSCSHAQILQEKTKLLTAIVNKLMDINGILEGKEESAGK-  104
CeHV-5      DDFEVRFEPMLPRVYELLLPSLDARLNFVNAGQKYAAFLKYVHGECSSCSHAQILQEKTKLLTAIVNKLMDINGILEGKEESSGK-  107
BatBHV-2    NEPDIRFEPMLPKVYEIMLPSLDAKINLINVGQRHAAFLRHVYGSCGDCVHAEILRNKVKLLTVILTKLLDVNGILERKDNK----  109
TuHV-1      DEFPVAFEPMLPRVYEIMLPSLDARLNFVNVGRRHAAFLRYVYGERVDCEHAHIVREKTKLLTAILTKLLDVNGILERR-------  119
```

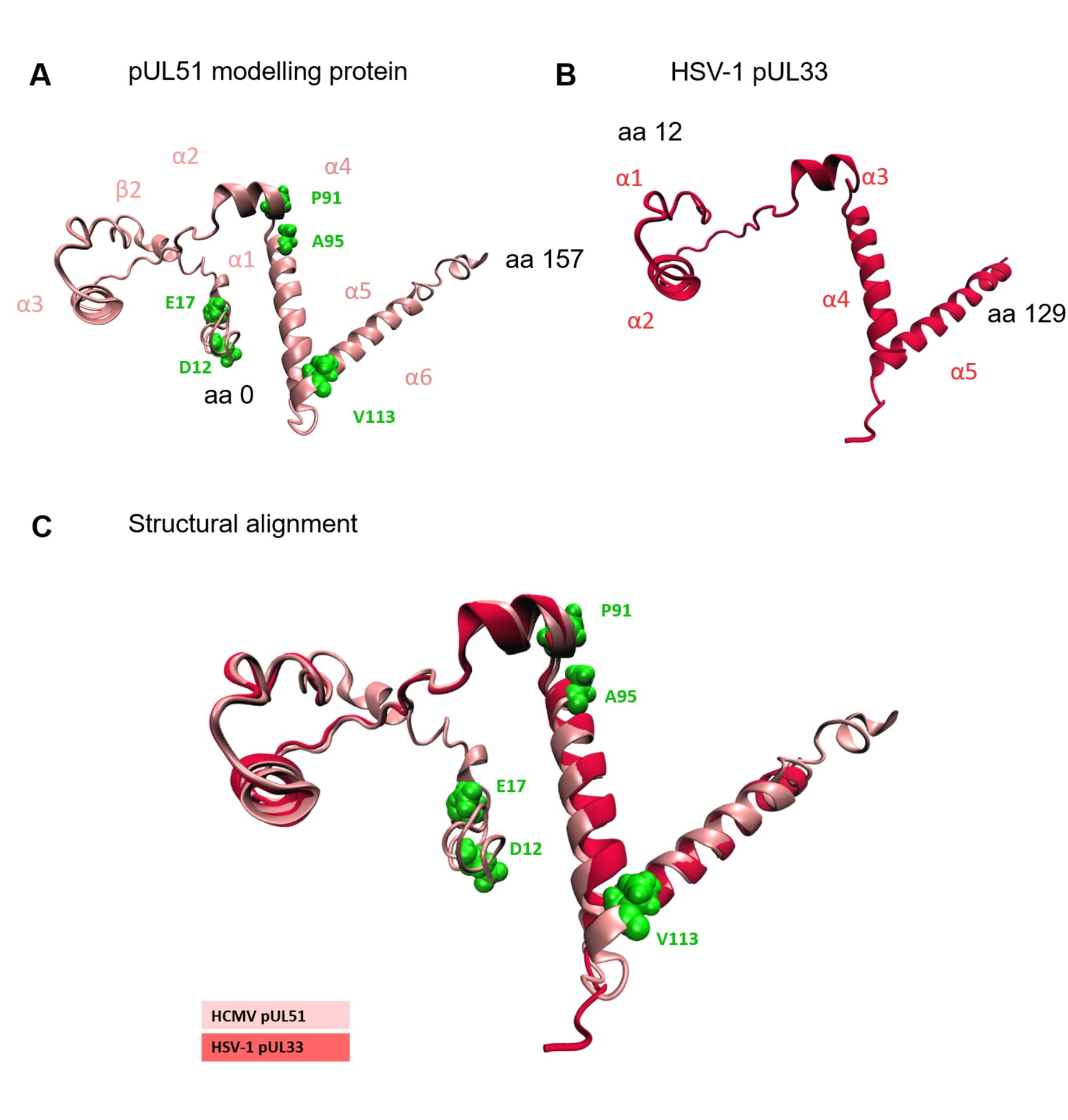
A
pUL51 modelling protein
α2
β2
α4
P91
A95
α1
α3
E17
α5
aa 157
D12
aa 0
α6
V113
B
HSV-1 pUL33
aa 12
α1
α3
α2
α4
aa 129
α5
C
Structural alignment
P91
A95
E17
D12
V113
HCMV pUL51
HSV-1 pUL33

HSV-1 pUL28
HSV-1 pUL15
HCMV pUL51

pUL51 A95

pUL28 D253
(L257)

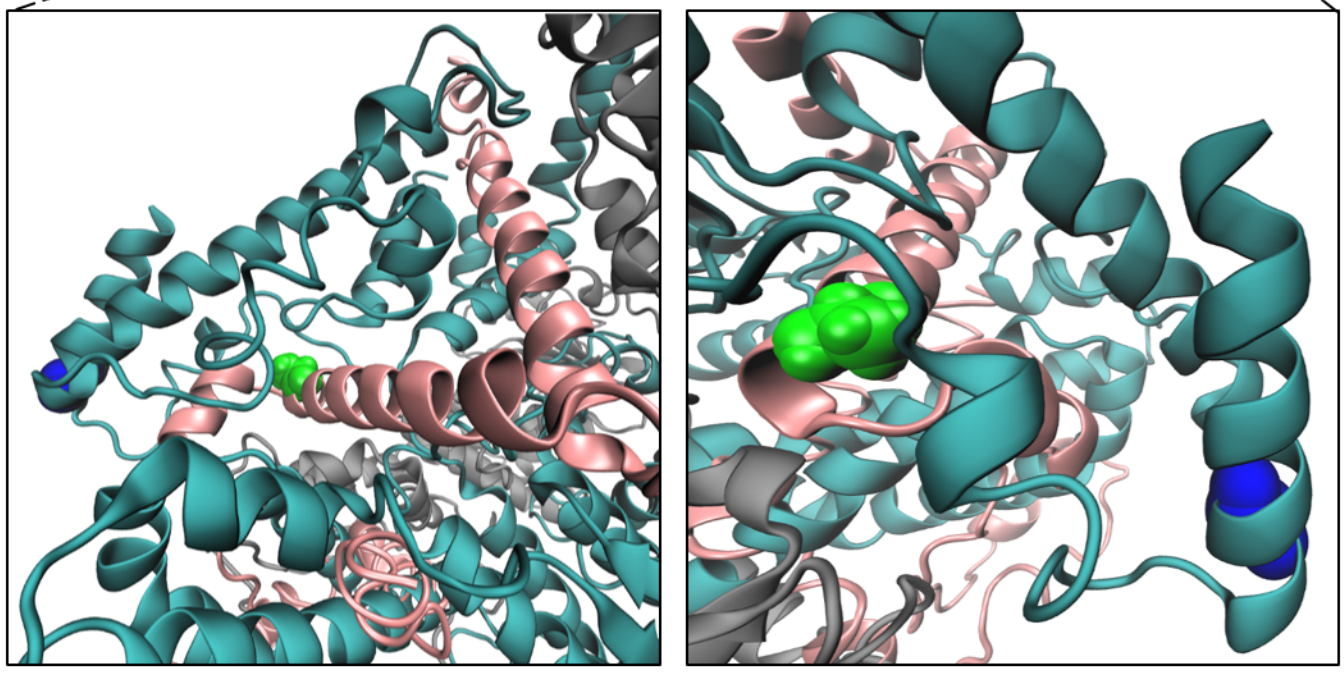

A

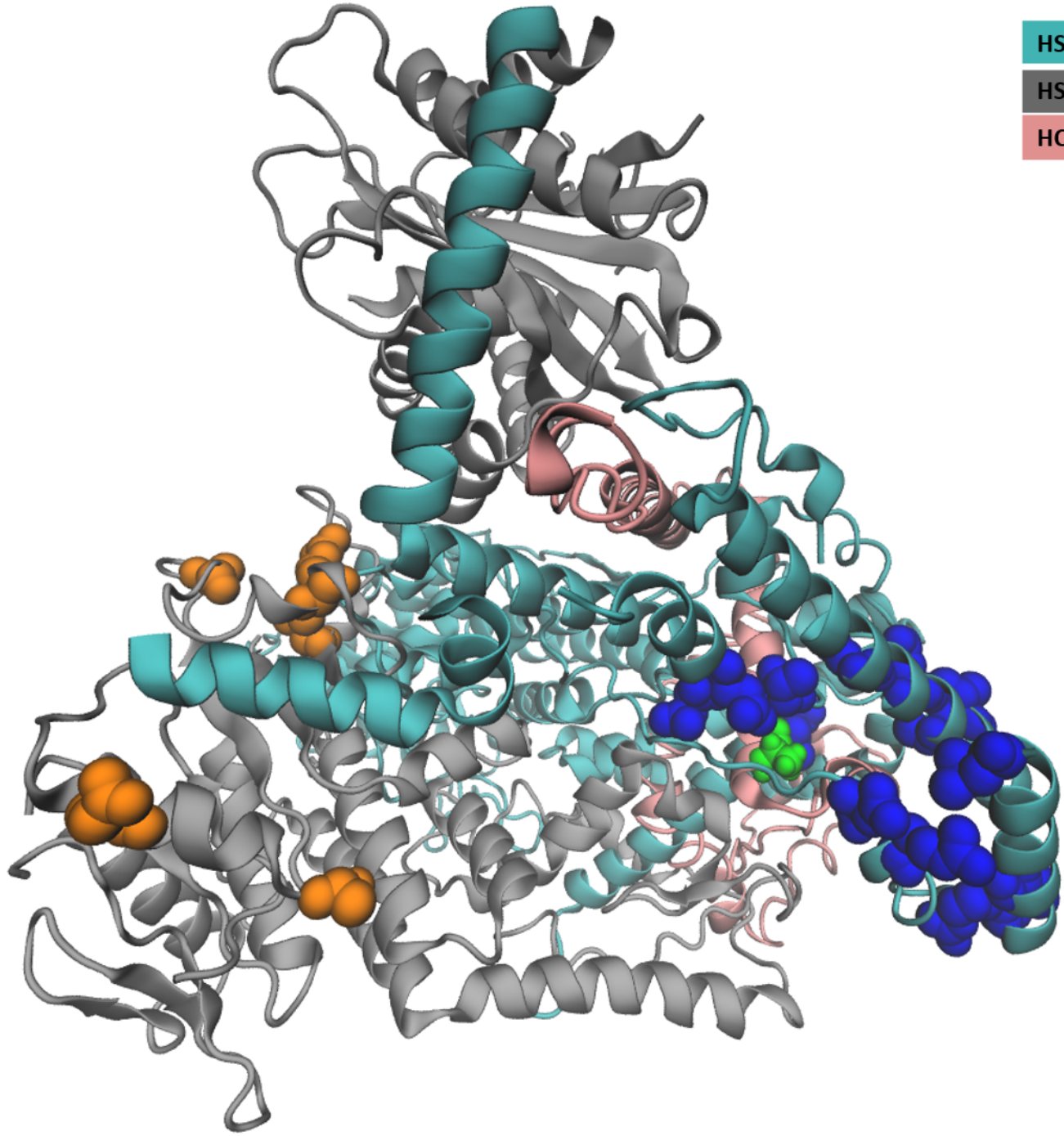

B

pUL56	C25	S229	V231	N232	V236	E237	L241	T244	L254	L257	K258	F261	Y321	C325	L328	M329	A365	N368	R369
pUL28	L31	/	/	/	/	/	N237	R240	S250	D253	R254	L265	R340	Q344	A347	A348	T386	D389	D390

pUL89	N320	N329	D344	T350	M359
pUL15	Q367	A376	A391	Y400	L409

Table 1 : Characteristics of the clinical samples

Accession numbers	UL56	UL89	UL51	Transplant	Treatment	Viral loads (log UI.mL^{-1})
ON505132	L257I	WT	A95V	HSC	LMV prophylaxis	3.21
ON505138	C325Y	WT	V113L	HSC	LMV prophylaxis	3.12
ON505141	C325F	WT	D12E	Kidney	LMV curative	3.40
ON505147	WT	WT	del17	Lungs	LMV curative	5.40

Table 2 : Effective Concentration 50% of viral growth (EC50) obtained for the recombinant viruses

Strains	Genotype		EC50 nM			
			LMV			
	UL51	UL56	Mean	SD[1]	N[2]	Ratio[3]
AD169	**WT**	**WT**	**2.123**	**0.633**	**7**	**1.0**
AD169	D12E	WT	3.018	0.373	3	1.4
AD169	17del	WT	2.878	0.339	3	1,3
AD169	A95V	WT	29.246	0.788	4	13.8
AD169	V113L	WT	3.206	0.453	4	1.5
AD169	D12E	C325F	>3000	/	4	
AD169	A95V	L257I	271.39	41.05	5	127.8
AD169	V113L	C325Y	>3000	/	3	

[1] Standard deviation of EC50 values
[2] Number of replicates of testing in triplicates (over at least 3 separate dates)
[3] Ratio of EC50 value to that of wild type control strain